# Robust Design of a Particle Free Silver-Organo-Complex Ink with High Conductivity and Inkjet Stability for Flexible Electronics

*Mohammad Vaseem*[*‡], Garret McKerricher[‡], and Atif Shamim*

IMPACT Lab, Computer, Electrical and Mathematical Sciences and Engineering Division, King Abdullah University of Science and Technology, Thuwal 23955-6900, Kingdom of Saudi Arabia

KEYWORDS: Silver-organo-complex (SOC) based ink, Inkjet printing, Jetting & storage stability, Reduction, Adhesion, Electrical conductivity, Inductors

**ABSTRACT**

Currently, silver nanoparticle based inkjet ink is commercially available. This type of ink has several serious problems such as a complex synthesis protocol, high cost, high sintering temperatures (~200 $^{0}$C), particle aggregation, nozzle clogging, poor shelf life, and jetting instability. For the emerging field of printed electronics, these short comings in conductive inks are barriers for their wide spread use in practical applications. Formulating particle free silver inks has potential to solve these issues, and requires careful design of the silver complexation. The ink complex must meet various requirements, such as in-situ reduction, optimum viscosity,

storage and jetting stability, smooth uniform sintered films, excellent adhesion, and high conductivity. This study presents a robust formulation of silver-organo-complex (SOC) ink, where complexing molecules act as reducing agents. The 17 weight percent silver loaded ink was printed and sintered on a wide range of substrates with uniform surface morphology and excellent adhesion. The jetting stability was monitored for 5 months to confirm that the ink was robust and highly stable with consistent jetting performance. Radio frequency inductors which are highly sensitive to metal quality were demonstrated as a proof of concept on flexible PEN substrate. This is a major step towards producing high quality electronic components with a robust inkjet printing process.

## INTRODUCTION

The field of printed electronics deals with several kinds of conductive inks, including nanoparticles, nanowire, and two-dimensional sheets, which are based on metal, silicon, carbon, and oxide semiconductors.[1-7] However, the printed electronics market is currently dominated by conductive metal nanoparticle based inks. The fabrication of high quality and low cost electronics requires innovative ink formulations that are cheaper and faster than traditional production methods. At present, most of the conductive inks available are based on silver nanoparticles, since silver possesses the highest conductivity without a difficult oxidation issue.[8-12] As a requirement, ink must be stable to aggregation and precipitation to achieve reproducible performance. To meet this requirement silver nanoparticle ink normally uses organic stabilizers; unfortunately the stabilizers also act as insulators.[12] Moreover, silver nanoparticle ink with a high solid content is more prone to stability issues, which generally result in clogging of the inkjet nozzles and concerns about shelf-life of the ink.[13] High silver loading is beneficial, but the high

temperature removal of organic stabilizers from the nanoparticles can limit the choice of the substrate. Thus, several other sintering techniques (e.g. intense pulsed light, UV-curing[14], microwave[15], photonic[16], and laser curing[17]) have been reported to lower the sintering temperature, while remaining compatible with polymer substrates. Although these methods are good alternatives, the simplicity and low cost of thermal sintering makes it a preferred choice. Fortunately, there is still ample room for tuning the ink chemistry to reduce the temperature.[8]

Compared to nanoparticles, metal-organo complex based ink has recently received significant attention as a potentially lower cost alternative that is stable at concentrations approaching saturation; neither additional stabilizers nor reducing agents are required.[18-19] Inkjet printing with the use of particle free metal-organic-complexes or salts of various metals is a very attractive low-cost technology for direct metallization.[20] By adjusting the viscosity and surface tension of the solution complex ink-chemistry, this type of ink could be used for various deposition techniques (e.g., spin-coating, direct ink writing, fine nozzle printing, airbrush spraying, inkjet-printing, screen printing, and roll-to-roll processing methods) in order to fabricate conductive tracks. A silver salt (20wt% silver) solution in methanol/anisole (ink purchased from TEC-IJ-040, InkTec Co., Ltd, Korea) was utilized by Perelaer et al. [21] Their study demonstrated that printed silver tracks on glass have a conductivity of 1.2-2.1×$10^7$ S/m at 150 $^0$C. Reactive silver inks, including ammonium hydroxide as a complexing agent and formic acid as a reducing agent, have been reported by Walker et al.[22] Such a reactive ink quickly decomposes, even at room temperature. Thus, it may not be suitable for a long-term inkjet printing process because it may lead to the formation of silver particles in the nozzle and clog it. In addition, fast vaporization of ammonia and carbon dioxide during the heating process leads to several bubbles. These gas bubbles from the vaporization of the silver ink components could drastically decrease the quality

of the silver film and interfere with adhesion of the silver to the substrate. Despite these possible drawbacks, this ink possessed the best conductivity at 90 °C, which is almost equivalent to that of bulk silver. Similar ink has been tested by Liu et al.[23] using laser direct patterning of silver film on polymer substrate. Chen et al.[24] spin-coated Ag(dien)](tmhd)/hexylamine/ethyl cellulose based ink on PI substrate, and then annealed it at 250 ºC for three hours; they obtained a conductivity of 1-2.1×$10^7$ S/m depending on film thickness. Recently, Dong et al.[25] synthesized MOC ink through a two-step process. First, silver oxalate was synthesized by silver nitrate and then dissolved in ethylamine as a complexing ligand, with ethyl alcohol and ethylene glycol as a solvent, using a low temperature (0 $^0$C) mixing process. The printed patterns on the PI substrate that were cured at 150 °C for 30 minutes showed metalized silver with a conductivity of 1.1×$10^7$ S/m.

The methods described above for formulating silver complex based ink suffer from several drawbacks. In some cases a multicomponent solvent in the ink has negative effects and the ink is less stable with poor electrical properties and film formation even at high-temperature annealing. In most of the reported SOC inks, adhesion with substrate is either not provided or discussed and jetting stability is not examined. For commercial utility, the design of silver complexation should meet the various requirements such as in situ reduction, optimal viscosity, storage & jetting stability, smooth uniform sintered films, and high conductivity. In the field of printed electronics, like other emerging electronic technologies, new materials and processing methods are required for their ever-improving development and performance.

In this study, we developed a novel SOC ink, a silver-ethylamine-ethanolamine-formate-complex based transparent and stable ink, wherein ethylamine, ethanolamine, and formate species act as in situ complexing solvents and reducing agents. As-formulated ink was inkjet

printed on a wide range of substrates, including PI, PET, PEN, and glass. The decomposition of ink led to uniform surface morphology with excellent adhesion to the substrates. The jetting and storage stability was monitored, which confirmed that the inks were highly stable with jetting for repeated performance. Combining these characteristics with the high conductivity of the ink, fabricated RF inductors demonstrated the best performance by inkjet printing to date. Inductor values up to 35nH with quality factors greater than 10 at frequencies above 1.5GHz prove the viability of the ink for the fabrication of printed electronics.

## RESULTS AND DISCUSSION

**Ink Chemistry:** The as-formulated ink is free of particles and is stable in a sealed glass vial at room temperature. However, storage stability can be extended if the ink is stored in an opaque vial and refrigerated at 4 $^{0}$C. The inks were prepared through the complexation between silver acetate and pH controlled complexing solutions. The complexing solutions contained ethylamines, ethanolamines, acetate anions, and formate anions. The lone pairs of electrons on the nitrogen atoms of ethylamine and ethanolamine can coordinate with silver cations and they may form Ag(ethylamine-ethanolamine) complexes that are balanced with formate anions (Fig. 1a). Usually, silver-amines complexes have very high solution pH (pH=13-14) and could not be used for effective reduction and decomposition but with the addition of formic acid and adjustment of solution pH to 10.5, the resultant ink has good stability and easy decomposition at elevated temperature. It should be noted that pH 10.5 is our optimized solution pH and provides the best chemical stability. However, further reduction of the solution pH may lead to instability and lower silver loading. Thus, we have concluded that both amine combinations are important not only for chemical stability but also for its decomposition at lower temperature with high conductivity. As the ink is heated above 80°C, elemental silver is the only phase that remains.

Pure elemental silver results from the decomposition and reduction of complexes by the formate anion, which leads to the slow evaporation of ammonia and carbon oxide along with the low boiling point reactants (Fig. 1b).

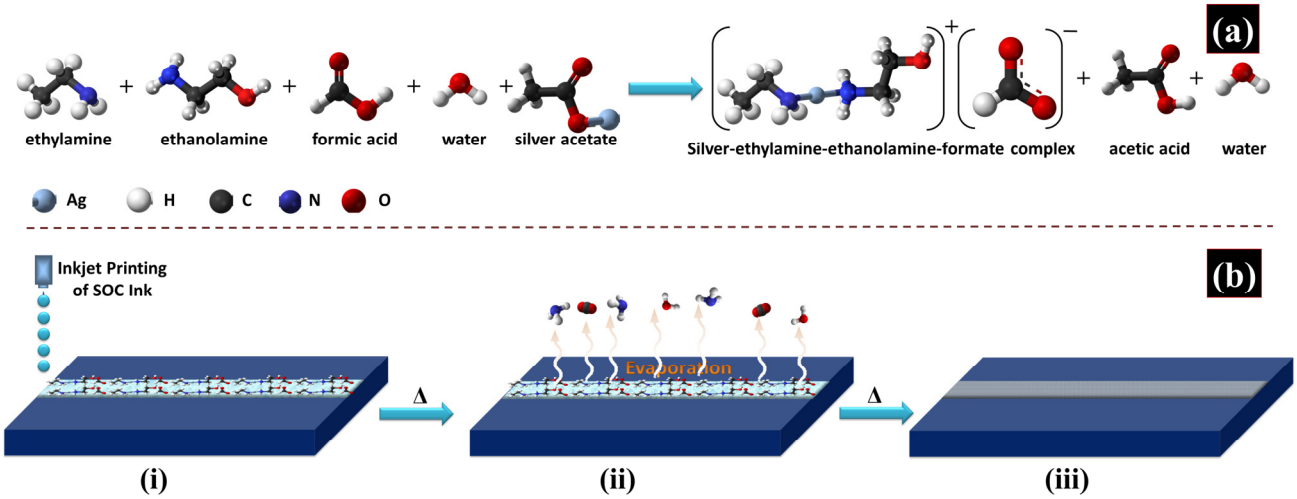


**Figure 1.** An illustrative procedure for the formulation of silver-ethylamine-ethanolamine-formate-complex based SOC ink. (a) Chemical reaction involved in the formulation of ink. (b) Schematic presentation of thermal reduction process for printed ink conversion to silver metallic phase and chemical reaction represented by ball-and-stick model.

To assess the quality of the ink, jetting stability and final film quality were investigated. Thus, the ink was formulated in such a way that the constituent solvent not only acts as a complexing and reducing agent, it also provides a more optimal viscosity and surface tension for ink jetting performance. Initially, the as-formulated ink had a viscosity of ~$4.95\times10^{-3}$ Pa.s and a surface tension of 33.08 mN/m, which is adequate for jetting. With the addition of 2-HEC, the ink demonstrated enhanced viscosity of ~$5.97\times10^{-3}$ Pa.s and reduced surface tension of 30.7 mN/m providing good jetting while improving adhesion. We investigated several solvents for use as an adhesive promotor, such as 2% hydroxyethylcellulose (HEC), 2% 2-hydroxyethylcellulose, 2, 3 butanediol, glycerol, ethylene glycol. It is observed that even without any additive, ink possesses

good adhesion on substrates and has good jetting and storage stability but with the adhesive promotor like cellulose (i.e. 2-HEC or HEC), it shows excellent adhesion as compare to glycol based additive or no additive (Please see supporting information Table S1). It is well documented that cellulose based molecules possess self-adhesion. Several theories have been proposed to provide an explanation for the adhesion phenomenon such as adsorption, electrostatic attraction and diffusion; however, there is no single theory that explains adhesion in general, as has been discussed in literature.[26] Further discussion on nanoparticle based film's adhesion to substrates through adhesion promotors can be found in references.[27,28] As can be seen in the above mentioned papers, the adhesion enhancement phenomenon due to promotors is a complex issue and can be explained based on multiple theories. In our case, a possible reason can be that the ink with promotor shows good wettability on the substrate, and it could be presumed that the physical adsorption due to van der Waals attraction force and acid-base interactions is contributing to the adhesion forces. However, detail investigation is further needed to explain this aspect in a more precise manner. It was realized that water compatible hydroxyethyl cellulose (HEC) is the best choice for our ink-formulation even with 2 wt% of it provides sufficient viscosity. All of the ink was jetted successfully, except for ink with 2% HEC. It is observed that even at high voltage with an efficient waveform the fluid is driven out of the orifice but then recoils back inside. It is believed that the high molecular weight and longer chain length of HEC is responsible for the problem; switching to shorter chain 2-HEC (MW-90000) exhibits excellent jetting behavior.

**Thermal Analysis of Ink:** The thermal decomposition of the ink and the Fourier transform-infrared (FT-IR) spectra of gas evolution during the process were determined using a thermogravimetric analysis infrared (TGA-IR). Figures 2a, 2b, and 2c show the TG- Gram

Schmidt curves, differential scanning calorimetry (DSC) curves, and FT-IR scans of the SOC ink, respectively. Fig. 2a shows the continuous weight loss, which starts at room-temperature and ends at ~162 $^{0}$C. The DSC curve shows an endothermic peak maximum at 148 $^{0}$C, corresponding to the final thermal decomposition of SOC ink.

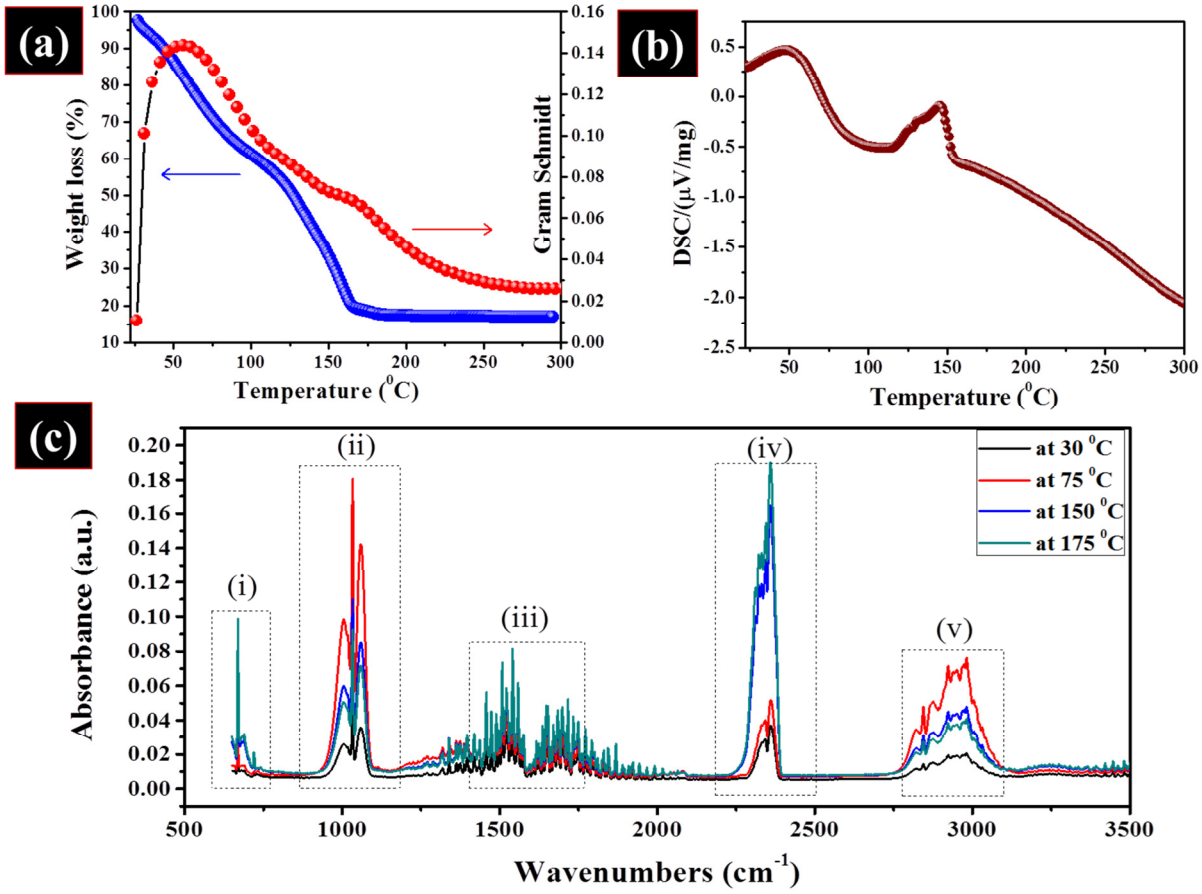


**Figure 2.** TGA and DSC analysis of the SOC ink (a) TGA and Gram Schmidt curves for the ink thermally sweep from room temperature to 300 $^{0}$C in air, (b) DSC curve from RT to 300 $^{0}$C and (c) FT-IR spectrum for in situ gas evolution during thermal decomposition.

A two-step weight loss was observed from the TG curve. The first step was completed at ~90 $^{0}$C. This step was characterized by a broad exothermic region on the DSC curve, which was

attributed to the evaporation of the low boiling solvents. The second step was completed at ~90 to ~160 $^0$C and was characterized by an endothermic region indicating the decomposition of the silver complex. The Gram Schmidt curve shows major gas evolved with broad peak maxima at ~55 and a low intensity peak at 150-175 $^0$C. Its corresponding FTIR scan shows that methanol is evaporated when the ink is heated in the range of room temperature to ~100 $^0$C. The peak region of (ii) corresponds to the methanol evaporation[29] with maximum absorption at 75 $^0$C, which is further reduced at higher temperatures. Regions (i) and (iii) show characteristics peaks for $NH_2$ scissoring (1550-1650 $cm^{-1}$) and $NH_2$ and N-H wagging (660 $cm^{-1}$), which corresponds to the evolution of ammonia.[25] The FT-IR scan also indicates prominent carbon dioxide gas evolution (region iv, 2230-2400 $cm^{-1}$)[30] with heating between ~150 and ~175 $^0$C, confirming that the ink completely decomposed at the second stage in the TG curve for the formation of metallic silver. Region (v) corresponds to the $–CH_2$ and $–CH_3$ stretching vibration, which could be a part of ethylamine and ethanolamine decomposition.[31] No further weight loss occurs at annealing temperatures above 150 $^0$C. Thus, sintering temperature was set at 150 $^0$C for conductivity measurements.

**Storage and Jetting Stability of Ink:** Particle free ink was formulated which does not aggregate or clog during printing. The ink provides both jetting stability and long term storage. The ink storage stability was monitored using a UV-Vis spectrophotometer. As shown in Fig. 3a, the absorption spectra from inks are featureless. Moreover, the absorption spectra shows weak absorption in the 400-425 nm range, where absorption is typically associated with the presence of silver particles (0.1% DGP-40LT silver NPs ink). This finding confirms that the ink was particle-free. After one month of storage, there was no sign of silver formation in the UV spectrum and the ink remained transparent. To confirm it more precisely, rheological

measurement of the ink was also examined and its related data is presented as supporting information Fig. S1. The graphs clearly show that there is no substantial change in viscosity with storage time (2 to 3 week) when applying shear rate of 0.1-1200 1/s. To provide further insight with storage and jetting stability, the evaporation rate of the ink has been investigated by thermogravimetric analysis and presented in supporting information Fig. S2. The ink was kept at different isothermal temperatures i.e. 28, 80 and 150 $^{0}$C for a period of time in constant air flow (20 mL/min) environment. However, it is worth mentioning here that these test conditions are not true representation of the ink in the cartridge, where ink is not much exposed and do not have operating cartridge temperature more than 60 $^{0}$C. As expected, the evaporation rate of the solvents at 28 $^{0}$C is much slower than 80 and 150 $^{0}$C. More than 50 % of the ink constituent retain over the period of 6 h. However, when the isothermal temperature is increased to 80 and 150 $^{0}$C, inks evaporate completely with faster rates (150 $^{0}$C within 30 min and 80 $^{0}$C in 2 h). It could be assumed that complete evaporation at 80 $^{0}$C needs more time than usual.

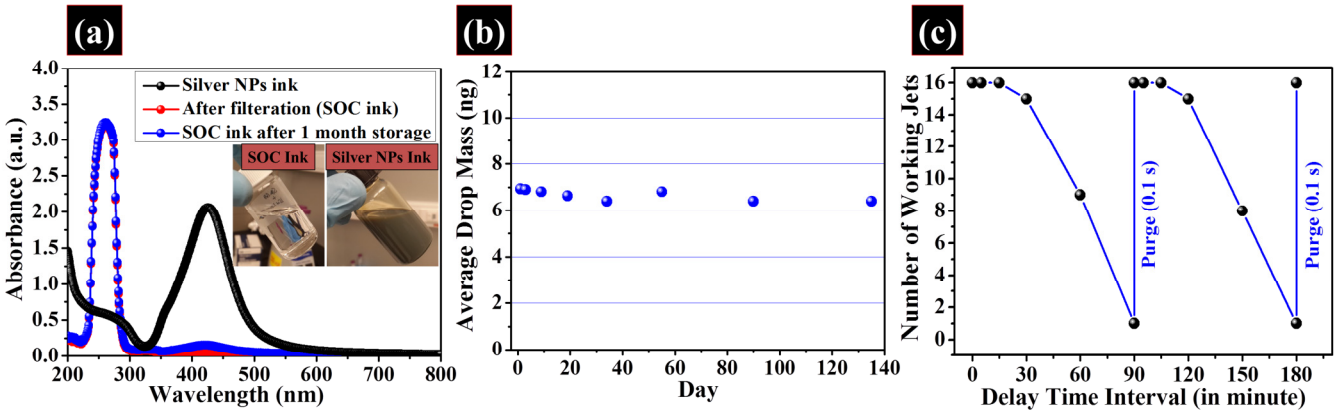


**Figure 3.** (a) Ink-storage monitored by ultraviolet-visible (UV-Vis) spectrophotometer and Ink-jetting stability for 10 pL cartridge monitored by evaluating (b) average drop mass with number of days and (c) number of working jets with delay time interval. For storage, the ink was kept in

a refrigerator at 4 $^{0}$C. The inset in spectrum (a) showing photographic image of ink sample and its comparison with nanoparticle based ink (Silverjet DGP-40LT). Jetting stability test confirmed that inks are highly stable with jetting for repeated performance.

Apart from ink storage stability, it is important to investigate the ink's jetting stability with time using conventional 10 pL nozzle as well as with 1 pL nozzle. Evaporation of the ink in the nozzle leads to clogging of the head as well as a decrease in drop mass over time. There are several reports [22-25] where authors have presented particle free ink-formulations, but none report jetting stability over time. If the ink is very reactive, such as silver-amino complex based reactive ink that can decompose even at room-temperature, then there is a chance of the ink drying in the nozzle.[22] However, in our ink-formulation low and high boiling amines not only complex with silver, they act as a co-solvent to suppress the evaporation rate. Methanol is added to adjust the surface tension (30.7± 0.5) of the ink which is almost stable over a time, thus stabilizing the ink performance. Fig. 3b shows a graph of the average drop mass monitored over 5 months for 10 pL nozzles, which was fairly consistent at just under 7 ng. The nozzles with 1pL also show consistent average drop mass of less than 1.25 ng over 3 week time (see Supporting Information Fig. S3a). This finding confirms that the ink is highly stable with jetting for repeated performance. The effect that delay time interval has on the number of working jets was also investigated, as presented in Fig. 3c. The number of working nozzle means that when the delay test starts there are total 16 nozzles available which drop the ink continuously. With every delay time interval, nozzles are paused and re-played and the working ability of the nozzles is assessed. Up to 30 minutes of delay, almost all the nozzles worked well but as the delay time interval increases from 30 to 60 mins, working nozzles dropped to total of 9, which further dropped to 1 after 90 min delay. Most of the nozzles stop working after a 90 min delay and the likely reason is

the evaporation of ink in the nozzle. However, after 0.1 s purge, all 16 nozzles again restart and follow the same delay trends. This may not be an issue in an industrial printing environment, since after a short purge (0.1 seconds) all jets return to the initial working state. Interestingly, delay test with 1pL nozzle shows much better performance than 10 pL nozzle (see Supporting Information Fig. S3a). Up to 180 minutes of delay, only 2 nozzles stopped working and rest of the nozzles worked perfectly. The reason is obvious as due to less opening of nozzle (9µm) evaporation of ink is much restricted in the nozzle.

**Morphological & Electrical Evolution of Printed Silver Film as a Function of Thermal Sintering:**

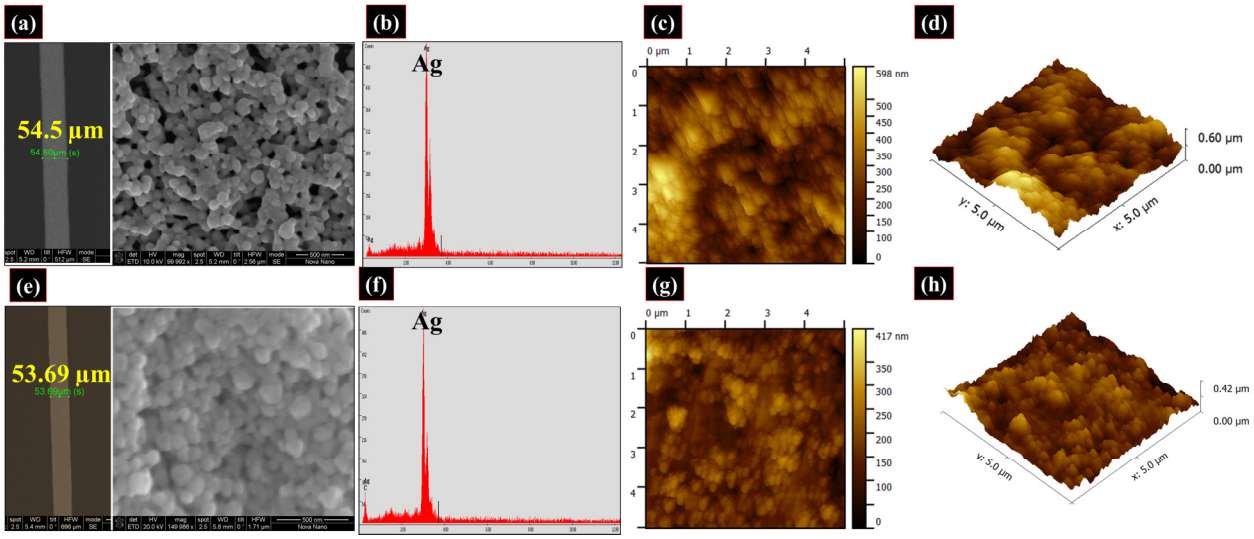


**Figure 4.** Inkjet-printed line pattern. SEM image and its corresponding EDS analysis, surface and 3D AFM topography for the films printed on (a-d) glass and (e-h) PEN. The samples were sintered at 150 $^{0}$C/30min.

Fig. 4 shows SEM, EDS analysis and AFM images of SOC ink printed on glass and PEN (*t*= 125 µm) substrate. The images clearly show that as-sintered particles are interconnected with

each other and they satisfy a three-dimensionally interconnected conduction pathway via inter-particle neck growth with a sintering temperature of 150 $^0$C/30 min. The printed silver line on the glass has a line width of ~54 μm (a). The EDS spectrum demonstrated that the as-sintered films are made of silver only without any impurities (b). AFM topography of the printed film clearly shows that as-sintered films were densified without any structural defects, with a root-mean-square (RMS) roughness of ~94.7 nm (c & d). In contrast to printing on glass, the silver line width of ~53 μm on PEN has less connected smaller particles with silver as an elemental phase (e-f) and with a roughness of ~44.5 nm (g-h). Figure S4 Supporting Information shows X-ray diffraction graphs of the printed films on glass and PEN substrates. The observed diffraction peaks are well match and indexed to face-centered cubic silver (JCPDS NO. 04-0783).[32] The strong and sharp peaks indicate that the silver films are highly crystalline and sintered.

To evaluate the electrical performance of SOC ink on glass and PEN substrate, 5×0.25 mm electrode lines were printed as a function of the over-printing number. Sintering was performed at 150 $^0$C for 30 minutes after printing each layer. Figures 5 (c) and 5 (d) show width scan profile graphs and an SEM image of the printed lines. The thickness of printed electrodes increases in a fairly linear manner with the number of printed layers. Figures 5 (a) and 5 (b) show graphs illustrating 4-point DC probe measured resistance and calculated electrical conductivity as a function of the number of over-printing layers on both glass and PEN substrates. Initially, single printing demonstrated conductivities of ~$0.66\times10^7$ and ~$0.4\times10^7$ S/m on glass and PEN, respectively. Differences in conductivity on different substrates are frequently observed.[33,34] To investigate the conductivity difference on glass and PEN substrates, we have checked cross-sectional SEM images and it is observed that the first layer of the printed film on PEN substrate has not been sintered well, as nano-particles in the underlying layer can be clearly seen (marked

with an arrow in Fig. S5 e-h). This is probably due to the lower thermal conductivity of PEN as compared to the glass substrate. However, with the amount of over-printing the conductivities substantially increased. With single printing and sintering, due to the presence of voids between

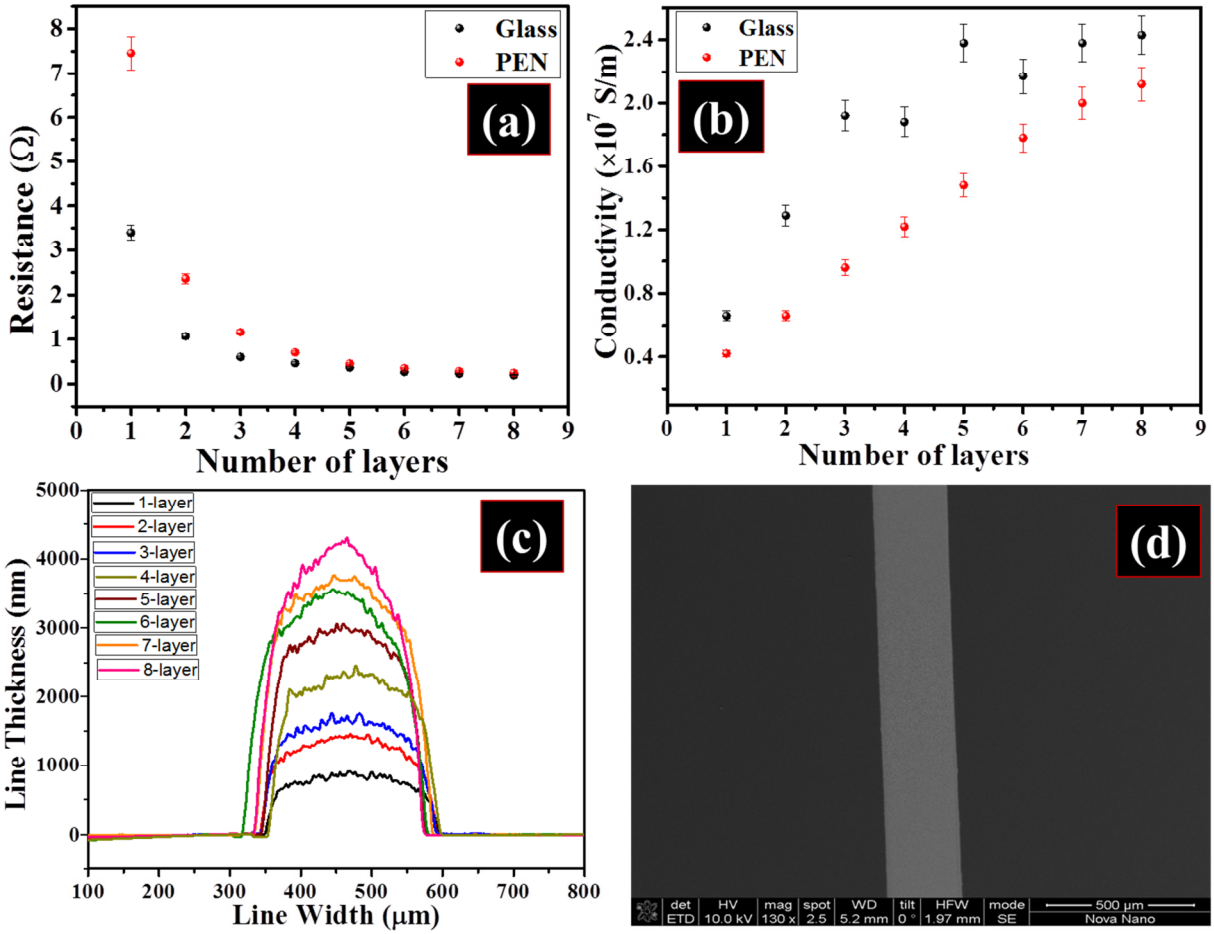


**Figure 5.** (a) Resistance of 5×0.25 mm lines as a function of printed layers (b) calculated conductivity as a function of overprints (c) profiles of printed lines versus printed layers on glass substrate (d) SEM image of a printed line on glass after being sintered at 150 $^{0}$C/30min.

the films, percolated conductive pathways may have been limited. Since the ink is particle free and has a liquid-like behavior, when it was over-printed on sintered film it went deep into the film and filled the voids after sintering and enhanced three-dimensional interconnection. Cross-

sectional SEM images of over-printed lines on glass and PEN substrates clearly show that the voids in the film have been filled (see Supporting Information Fig. S5). With printing numbers of seven to eight, the conductivity became saturated at ~$2.43\times10^7$ and ~$2.12\times10^7$ S/m on glass and PEN, respectively. The previously reported reactive silver ink[22] has higher conductivity as highlighted in Supporting information, Table S2. Table S2 compares the performance properties of several other SOC and nanoparticle inks and considering all requirements on jetting stability, adhesion, and storage, this ink distinguishes itself from other works.

**Adhesion Test of Printed Silver Film to Hard & Soft Substrates:** The adhesion of the printed ink to several substrates, including glass, polyimide, and PET films, was assessed. Scotch tape was used to test adhesion by applying tape to the entire region of the each silver film. After removing the tape, the samples were inspected visually to determine the amount of silver that was removed from the substrate. It was observed that the ink possessed excellent adherence to all of the substrates without any post resistance change. All plastic films were also stressed and bent with no observed decrease in adhesion of the silver film or any change in resistance. All of the examinations are demonstrated in the supplementary video V1.

**Inkjet-printing Smaller Features:** Due to the particle free nature of this SOC ink and the excellent performance through a conventional inkjet nozzle (10pL) presented in the previous sections, a smaller nozzle (1pL) has been successfully tested without any clogging or flow issues. The spreading and drying of SOC ink is not inhibited by particles and needs to be carefully controlled to obtain fine features. The minimum printed feature sizes and gaps were investigated, which are of interest in electronics design. For printing narrow line traces, substrate surface energy should be uniform throughout the substrate area. To create uniform surfaces, glass substrate was spin-coated (5000 rpm for 40s) with a layer of PVP with thickness of ~100 nm

(5wt% in 1-hexanol with 0.77 wt% of crosslinking agent poly (melamine-co-formaldehyde) and heated at 180 $^{0}$C for 10 minutes prior to printing. Fig. 6 shows microscopic images of printed line tracks using 20 µm drop-spacing, which resulted in minimum line spacing of ~40 (a & b) and ~18 µm (c & d) with a line width of ~20 µm. These are encouraging results for any inkjet-printed electronic applications which require small feature sizes.

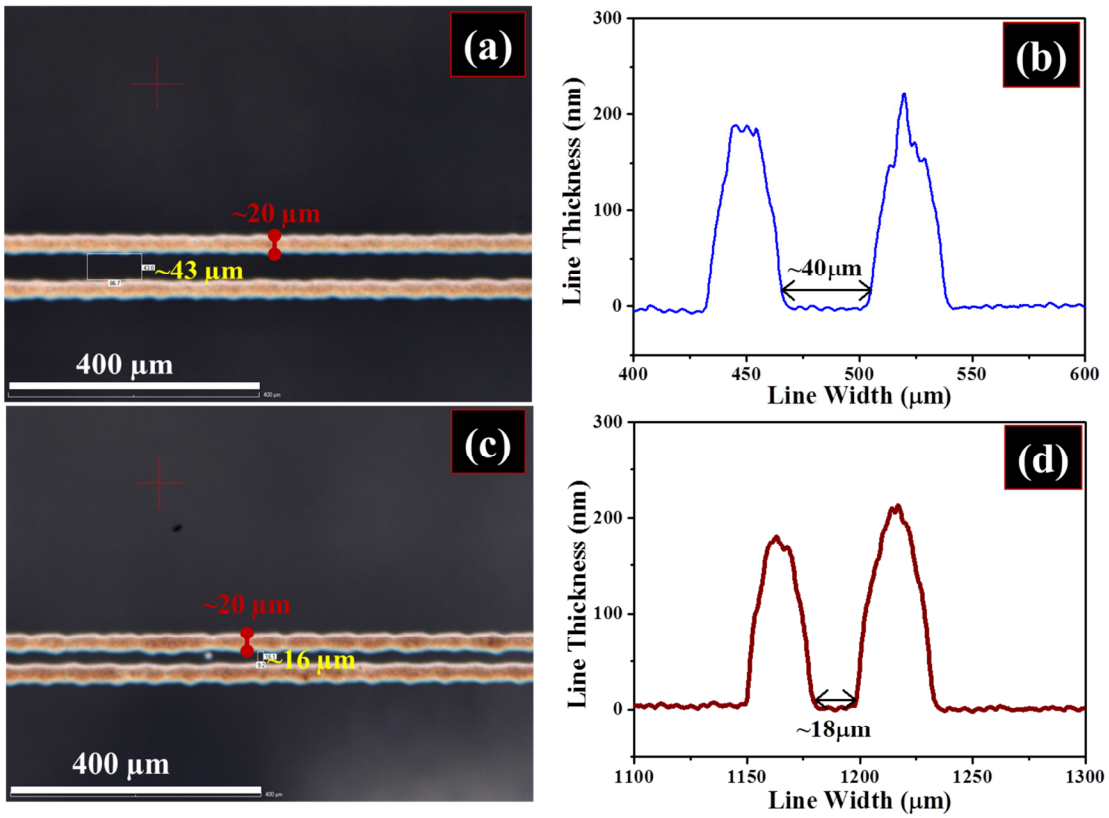


**Figure 6.** Printed narrower lines using 1 pL nozzle sintered at 150 $^{0}$C/30min. (a) microscope image of 40µm gap (b) profile of the 40µm gap, (c) microscope image of 18µm gap, (d) Profile of 18µm gap.

**Inkjet-printed RF Inductors:** There have been several reports of RF inductors [35-38], however due to the sensitivity to metal conductivity, thickness, and roughness, high quality inkjet-printed RF inductors remain elusive. RF inductors are a fundamental building block in circuits. Planar spiral inductors are common and Intel corp. has demonstrated inductors with quality factors (Q's) greater than 20, utilizing 8 μm of highly conductive metal.[39] Surface mount wire wound inductors are more complex to fabricate and they require mounting. However, they provide unrivaled performance, with inductance values greater than 10 nH and quality factors greater than 50.[40] Inductance values larger than one or two nH are physically large and are typically placed off chip; these would benefit the most from a printing technique. The pioneering work on inkjet-printed inductors demonstrates quality factors of ~0.5.[35] More recently, meander inductors and fully printed inductors have been shown with Q's approaching five.[36, 37] A 25 nH inductor with a Q approaching nine was also shown in 2014.[38] All of these printed inductors utilize nanoparticle ink as well as a sintering temperature greater than 150 $^{0}$C. In order to make repeatable, quality RF components by inkjet, a robust metal ink with high conductivity is required. The SOC ink developed here presents improved performance over nanoparticle ink and provides high value inductors with quality factors approaching 15. A depiction of the dimensions of the inductors as well as an image of the printed inductor is shown in Fig. 7.

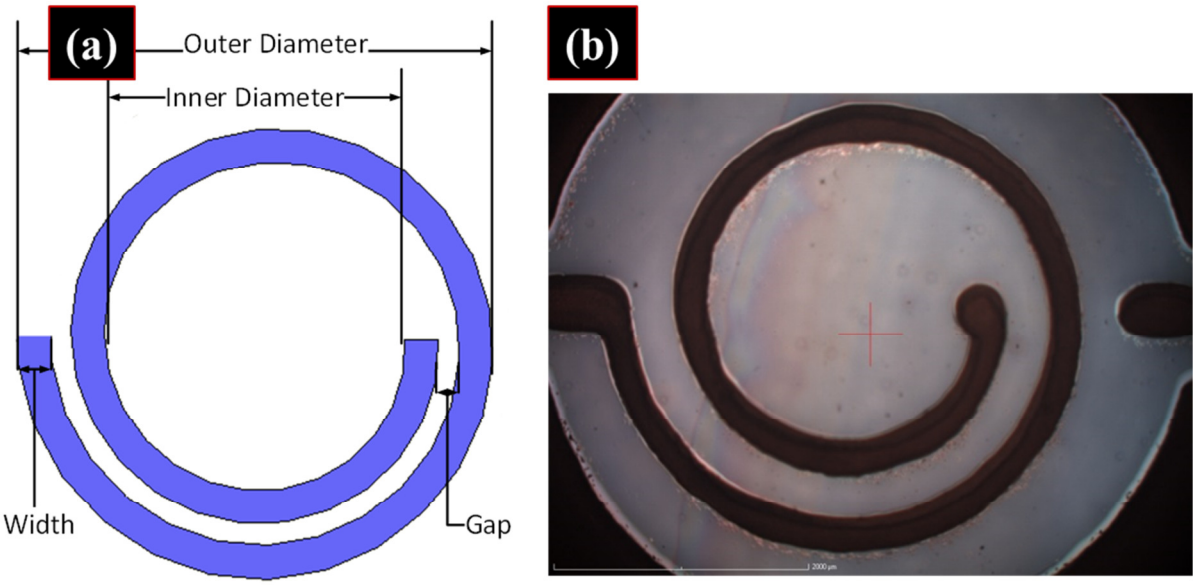


**Figure 7.** (a) Depiction of the inductor with dimensions (b) Microscope image of printed inductor

Spiral inductors are designed with Ansoft High Frequency Structure Simulator software and both a one and a half turn and a two and a half turn inductor are fabricated. The devices are measured with a network analyzer into the GHz regime, and the measured S-parameters from the analyzer are converted to Y-parameters.[41] The return path and pads are de-embedded using a standard open short method to reduce parasitic effects.[41] After de-embedding, the inductance and quality factor are calculated using equations (1) and (2).

$$L = \frac{im\left(\frac{4}{Y_{11} + Y_{22} - Y_{12} - Y_{21}}\right)}{2\pi f} \quad (1)$$

$$Q = -\left(\frac{im(Y_{11} + Y_{22} - Y_{12} - Y_{21})}{re(Y_{11} + Y_{22} - Y_{12} - Y_{21})}\right) \quad (2)$$

The dimensions of the inductors along with the measured parameters of inductance, quality factors, and self-resonant frequencies are highlighted in Table I.

Table 1

MEASURED INDUCTORS

| **Dimensions** | | | | | **Measured** | | |
|---|---|---|---|---|---|---|---|
| Turn | Outer Diameter (mm) | Inner Diameter (mm) | Gap (μm) | Width (μm) | L (nH) | QF (max) | SRF (GHz) |
| 1.5 | 3.7 | 2.0 | 200 | 350 | 10.5 | 15 | 4 |
| 2.5 | 5.6 | 3.0 | 200 | 350 | 35.5 | 11 | 1.5 |

L = inductance, QF =quality factor, SRF = self-resonant frequency

The electromagnetic simulations show a good match to the measured inductance values in Fig. 8. Two inductors were fabricated of each size validating the repeatability of the process. The measured inductors show quality factors above ten, which is considered state of the art for printed inductors. This is a step forward in making high quality components with a robust printing process.

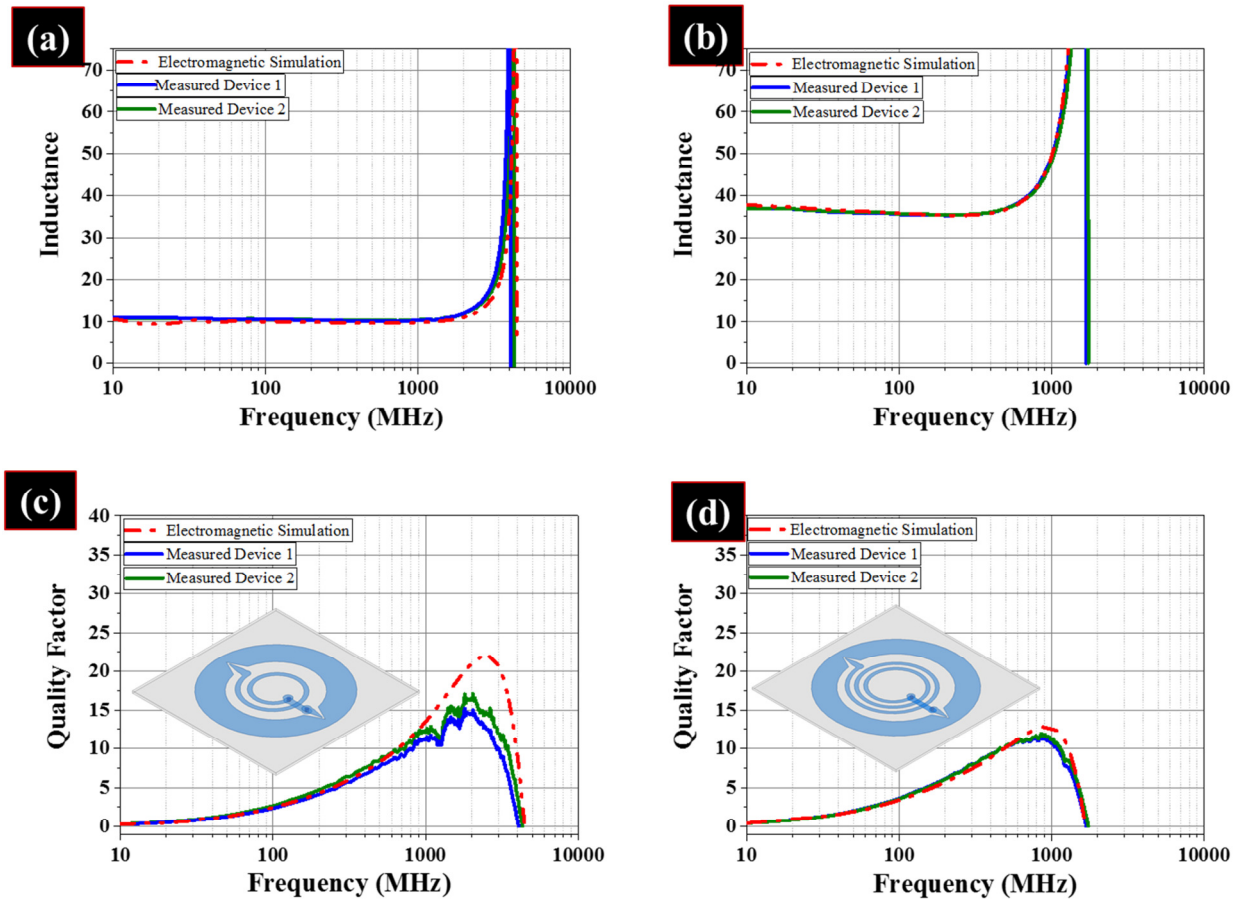


**Figure 8.** Inductance and quality factor versus frequency for printed inductors supported on PEN substrate: (a) 1.5 turn inductance (b) 2.5 turn inductance (c) 1.5 turn quality factor (d) 2.5 turn quality factor

## CONCLUSIONS

This work presents a detailed study of a novel type of SOC ink; namely, silver-ethylamine-ethanolamine-formate-complex based robust ink. SOC ink has the potential as a low cost alternative to nanoparticle based synthesis. It can provide high conductivities even at low temperatures ~ 150 $^{o}$C. It is particle free and has been shown to have stable jetting for more than 5 months. With appropriate additives the stable complexation is not disturbed and excellent adhesion to a wide variety of substrates is achieved. To demonstrate the capability of the ink, RF

inductors have been realized which are sensitive to the conductivity, thickness, and roughness of the printed metal. Ten to 35 nH inkjet-printed spiral inductors on flexible plastic have maximum quality factors greater than ten and self-resonant frequencies above 1.5 GHz. These are the first SOC inkjet-printed inductors and report superior performance over nanoparticle based devices even at a lower temperature. This robust ink formulation shows potential for high quality RF component fabrication as well as printed electronics in general.

## MATERIALS AND METHODS

***Chemicals*:** Silver acetate ($CH_3COOAg$, ReagentPlus®, 99%), ethylamine ($NH_2CH_2CH_3$, 2M in methanol, ACS reagent), ethanolamine ($NH_2CH_2CH_2OH$, ACS reagent, ≥99.0%), formic acid (HCOOH, reagent grade, ≥95.0%), and 2-hydroxyethylcellulose (2-HEC, MW=90,000) were used as they were received, without further purification.

***Ink-formulation:*** In an illustrative experiment, a 2M ethylamine solution in methanol, which was called as "Complexing Solution #1" was put in a vial. 10 mL of ethanolamine and 10 mL of deionized (DI) water (1:1 ratio) was mixed in another a vial. Formic acid ($\eta$=1.78 mPa s, $\gamma$=37.67 mN/m, $T_b$=100.8 $^0$C) was then added to the solution in a drop-wise manner to adjust the solution to pH 10.5. The resulting solution was called "Complexing Solution #2". In another vial, 1g of silver acetate was vortex mixed with 2 mL of complexing solution #1, 1.5 mL of complexing solution #2, and 0.5 mL of 2% 2-hydroxyethylcellulose (2% 2-HEC in water: methanol) at room-temperature for 30 seconds, resulting in a light black colored solution. This finding demonstrates that 2-HEC not only acts as viscofier, it also acts as an additive for adhesion of the ink to the substrate. The as-obtained solution was then kept for twelve hours to allow any particles to settle out, yielding a clear supernatant, which was decanted and filtered through a 200 nm syringe

filter. This clear and transparent solution that contains approximately ~17 wt% silver, served as the silver-ethylamine-ethanolamine-formate complex based SOC ink.

***Inkjet-printing of SOC ink:*** The as-formulated SOC ink was inkjet-printed on various substrates using a drop-on-demand piezoelectric ink-jet nozzle (manufactured by Dimatix) with a diameter of 21 and 9 µm and drop volume of 10 and 1 pL. The uniform and continuous ejection of droplets was achieved by adjusting various wave-forms while applying a firing voltage of 19-21 V at a 5 kHz printer velocity. To quantify the number of drops for jetting stability test, five jets were chosen and their drop velocities of 5000 drops/s were adjusted, which jetted continuously for 120 seconds. Subsequently, the total jetted drops were weighed and they correspond to the drop mass. Then, total drop mass was divided by number of drops, which provided the average drop mass in nano-grams. The ink droplets were dispensed with a spacing of 20 µm and several fine line patterns and electrodes (5 mm length and 0.25 mm width) were printed.

***Fabrication and measurement of printed inductors:*** The inductors were fabricated on PET substrate ($t$= 125 µm) using five layers of AOC ink at 20um drop spacing with a 10pL Dimatix DMP 2831 inkjet printer. The ink was heated at 150 $^0$C for 30 minutes in an oven after each layer was printed. A universal laser system PLS6.75 was utilized to cut via holes and make a connection with the underside of the inductors. Three layers of ink were printed to connect the vias and DuPont 5000 conductive paste and fill the laser drilled via holes. The inductors were measured in a two port configuration using 500 µm pitch Z-probes and a cascade probe station. An Agilent E8361A network analyzer was used to characterize the devices.

***Characterization:*** The structural properties were examined using scanning electron microscopy (FEI NovaNano FEG-SEM 630). The thickness and uniformity of printed features on substrates were performed using a surface profiler (Veeco Dektak 150), 3D interferometry (Zygo, Newview

7300) and cross-sectional SEM images. The film thickness on flexible PEN substrate was performed by milling through FIB tool (Quanta 3D FEG). Crystallinity of the silver film was examined by X-ray diffraction (Bruker D8 Advance) in the range of 20-80º at 40 kV. The UV-Vis absorption spectrum of the ink was obtained using a UV-Vis spectrophotometer (Cary 100 UV-Vis-NIR) with a standard 1 cm liquid cuvette, and with a background calibration run using deionized water. Surface tension and Rheology of the inks were measured using a KRUSS Tensiometer and Rheometer (Bohlin Gemini 2). Thermogravimetric analysis was performed using a TG 209 F1 analyzer (Netzsch), which was equipped with TGA-IR (Tensor 27, Bruker), at a temperature range of 25-300 $^{0}$C; it had a heating rate of 10 ºC/min in air flow. For isothermal thermogravimetric analysis, heating rate of 5 $^{0}$C/min was provided to reach the isothermal temperature. Differential scanning calorimetry (DSC) was observed by a STA 449 F1 (Netzsch) analyzer in nitrogen flow. Electrical resistances of silver electrodes were measured with a four-point probe method (Keithley 4200-SCS).

ASSOCIATED CONTENT

**Supporting Information**

Table consisting brief ink-formulation and its ink properties with different additives, a comparison table of conductivities obtained using various silver inks in the literature, rheology, thermogravimetric analysis for evaporation rate of the ink, jetting stability of the ink, cross-sectional SEM images of printed lines on substrates and X-ray diffraction graphs for inks printed on glass and PEN substrate. A video showing the adhesion tests of the ink to different substrates. This material is available free of charge via the Internet at http://pubs.acs.org.

AUTHOR INFORMATION

**Corresponding Author**

Correspondence and requests for materials should be addressed to M.V. (mohammad.vaseem@kaust.edu.sa)

**Author Contributions**

The manuscript was written through the contributions of all authors. All authors have given approval to the final version of the manuscript.

‡These authors contributed equally.

**Notes**

The authors declare no competing financial interests.

**ACKNOWLEDGMENTS**

We acknowledge financial support from King Abdullah University of Science and Technology (KAUST). Authors would like to thank Dr. Jose Gonzalez for his advice with electromagnetic simulation and measurements. Don Titterington and David Hustead from 3D Systems Willsonville, USA for sharing their industrial inkjet printing expertise. Muhammad Fahad Farooqui, Ahmad Nafe, and Shuai Yang from KAUST for their assistance with laser engraving, high frequency measurements and microscopic imaging. Authors also would like to thank Nini Wei from Core Lab facility for FIB analysis.

**REFERENCES**

(1) Lee, T. I.; Choi, W. J.; Moon, K. J.; Choi, J. H.; Kar, J. P.; Das, S. N.; Kim, Y. S.; Baik, H. K.; Myoung, J. M. Programmable Direct-Printing Nanowire Electronic Components. *Nano Lett.* **2010**, *10*, 1016-1021.

(2) An, K.; Hong, S.; Han, S.; Lee, H.; Yeo, J.; Ko, S. H. Selective Sintering of Metal

Nanoparticle Ink for Maskless Fabrication of an Electrode Micropattern Using a Spatially Modulated Laser Beam by a Digital Micromirror Device. *ACS Appl. Mater. Interfaces* **2014**, *6*, 2786-2790.

(3) Hamedi, M. M.; Hajian, A.; Fall, A. B.; Hakansson, K.; Salajkova, M.; Lundell, F.; Wagberg, L.; Berglund, L. A. Highly Conducting, Strong Nanocomposites Based on Nanocellulose-Assisted Aqueous Dispersions of Single-Wall Carbon Nanotubes. *ACS Nano* **2014**, *8*, 2467-2476.

(4) Lee, D.; Paeng, D.; Park, K.; Grigoropoulos, C. P. Vacuum-Free, Maskless Patterning of Ni Electrodes by Laser Reductive Sintering of NiO Nanoparticle Ink and Its Application to Transparent Conductors. *ACS Nano* **2014**, *8*, 9807-9814.

(5) Torrisi, F.; Hasan,T.; Wu, W.; Sun, Z.; Lombardo, A.; Kulmala, T. S.; Hsieh, G.-W.; Jung, S.; Bonaccorso, F.; Paul, P. J.; Chu, D.; Ferrari, A. C. Inkjet-Printed Graphene Electronics. *ACS Nano* **2012**, *6*, 2992-3006.

(6) Li, R.-Z.; Hu, A.; Zhang, T.; Oakes, K. D. Direct Writing on Paper of Foldable Capacitive Touch Pads with Silver Nanowire Inks. *ACS Appl. Mater. Interfaces* **2014**, *6*, 21721-21729.

(7) Ghosh, S.; Yang, R.; Kaumeyer, M.; Zorman, C. A.; Rowan, S. J.; Feng, P. X.-L.; Sankaran, R. M. Fabrication of Electrically Conductive Metal Patterns at the Surface of Polymer Films by Microplasma-Based Direct Writing. *ACS Appl. Mater. Interfaces* **2014**, *6*, 3099-3104.

(8) Magdassi, S.; Grouchko, M.; Berezin, O.; Kamyshny, A. Triggering the Sintering of Silver Nanoparticles at Room Temperature. *ACS Nano* **2010**, *4*, 1943-1948.

(9) Ladd, C.; So, J.-H.; Muth, J.; Dickey, M. D. 3D Printing of Free Standing Liquid Metal Microstructures. *Adv. Mater.* **2013**, *25*, 5081-5085.

(10) Diaz, E.; Ramon, E.; Carrabina, J. Inkjet Patterning of Multiline Intersections for Wirings in Printed Electronics. *Langmuir* **2013**, *29*, 12608-12614.

(11) Zheng, Y.; He, Z.-Z.; Yang, J.; Liu, J. Personal Electronics Printing via Tapping Mode Composite Liquid Metal Ink Delivery and Adhesion Mechanism. *Sci. Rep.* **2014**, *4*, 4588-4595.

(12) Kamyshny, A.; Magdassi, S. Conductive Nanomaterials for Printed Electronics. *Small* **2014**, *10*, 3515-3535.

(13) Ahn, B.; Duoss, E.; Motala, M.; Guo, X.; Park, S.; Xiong, Y.; Yoon, J.; Nuzzo, R.; Rogers, J.; Lewis, J. Omnidirectional Printing of Flexible, Stretchable, and Spanning Silver

Microelectrodes. *Science* **2009**, *323*, 1590-1593.

(14) Valeton, J. J. P.; Hermans, K.; Bastiaansen, C. W. M.; Broer, D. J.; Perelaer, J.; Schubert, U. S.; Crawford, G. P.; Smith, P. J. Room Temperature Preparation of Conductive Silver Features using Spin-coating and Inkjet Printing. *J. Mater. Chem.* **2010**, *20*, 543-546.

(15) Perelaer, J.; Jani, R.; Grouchko, M.; Kamyshny, A.; Magdassi, S.; Schubert, U. S. Plasma and Microwave Flash Sintering of a Tailored Silver Nanoparticle Ink, Yielding 60% Bulk Conductivity on Cost-Effective Polymer Foils. *Adv. Mater.* **2012**, *24*, 3993-3998.

(16) Perelaer, J.; Abbel, R.; Wünscher, S.; Jani, R.; Lammeren, T.; Schubert, U. S. Roll-to-Roll Compatible Sintering of Inkjet Printed Features by Photonic and Microwave Exposure: From Non-Conductive Ink to 40% Bulk Silver Conductivity in Less Than 15 Seconds. *Adv. Mater.* **2012**, *24*, 2620-2625.

(17) Liu, Y.-K.; Lee, M.-T. Laser Direct Synthesis and Patterning of Silver Nano/Microstructures on a Polymer Substrate. *ACS Appl. Mater. Interfaces* **2014**, *6*, 14576-14582.

(18) Lee, H. M.; Seo, J. Y.; Jung, A.; Choi, S.-Y.; Ko, S. H.; Jo, J.; Park, S. B.; Park, D. Long-Term Sustainable Aluminum Precursor Solution for Highly Conductive Thin Films on Rigid and Flexible Substrates. *ACS Appl. Mater. Interfaces* **2014**, *6*, 15480-15487.

(19) Shin, D.-H.; Woo, S.; Yem, H.; Cha, M.; Cho, S.; Kang, M.; Jeong, S.; Kim, Y.; Kang, K.; Piao, Y. A Self-Reducible and Alcohol-Soluble Copper-Based Metal-Organic Decomposition Ink for Printed Electronics. *ACS Appl. Mater. Interfaces* **2014**, *6*, 3312-3319.

(20) Kamyshny, A.; Steinke, J.; Magdassi, S. Metal-based Inkjet Inks for Printed Electronics. *TOAPJ* **2011**, *4*, 19-36.

(21) Perelaer, J.; Hendriks, C. E.; WM de Laat, A.; Schubert, U. S. One-step Inkjet Printing of Conductive Silver Tracks on Polymer Substrates. *Nanotechnology* **2009**, *20*, 165303-165307.

(22) Walker, S. B.; Lewis, J. A. Reactive Silver Inks for Patterning High-Conductivity Features at Mild Temperatures. *J. Am. Chem. Soc.* **2012**, *134*, 1419-1421.

(23) Liu, Y.-K.; Lee, M.-T. Laser Direct Synthesis and Patterning of Silver Nano/Microstructures on a Polymer Substrate. *ACS Appl. Mater. Interfaces* **2014**, *6*, 14576-14582.

(24) Chen, C.-N.; Dong, T.-Y.; Chang, T.-C.; Chen, M.-C.; Tsai, H.-L.; Hwang, W.-S. Solution based β-diketonate Silver Ink for Direct Printing of Highly Conductive Features on a Flexible Substrate. *J. Mater. Chem. C* **2013**, *1*, 5161-5168.

(25) Dong, Y.; Li, X.; Liu, S.; Zhu, Q.; Li, J.-G.; Sun, X. Facile Synthesis of High Silver Content MOD Ink by using Silver Oxalate Precursor for Inkjet Printing Applications. *Thin Solid Films* **2015**, *589*, 381-387.

(26) Gardner, D. J.; Oporto, G. S.; Mills, Ryan; Samir, M. A. S. A. Adhesion and Surface Issues in Cellulose and Nanocellulose. *J. Adhes. Sci. Technol.* **2008**, *22*, 545-567.

(27) Joo, S.; Baldwin, D. F. Adhesion Mechanisms of Nanoparticle Silver to Substrate Materials: Identification. *Nanotechnology* **2010**, *21*, 055204-055215.

(28) Cao, Z.; Stevens, M. J.; Dobrynin, A. V. Adhesion and Wetting of Nanoparticles on Soft Surfaces. *Macromolecules* **2014**, *47*, 3203-3209.

(29) Falk, M.; Whalley, E. Infrared Spectra of Methanol and Deuterated Methanols in Gas, Liquid, and Solid Phases. *J. Chem. Phys.* **1961**, *34*, 1554-1568.

(30) Zelayandia, O. Adsorbent for gases, WO2007022595 A1, March 1, **2007.**

(31) P. Larkin, *Infrared and Raman Spectroscopy Principles and Spectral Interpretation*, 1st ed; Elsevier Publications, Waltham, MA, USA **2011**.

(32) Vaseem, M.; Lee, K. M.; Hong, A-R.; Hahn, Y.-B. Inkjet Printed Fractal-Connected Electrodes with Silver Nanoparticle Ink. *ACS Appl. Mater. Interfaces* **2012**, *4*, 3300-3307.

(33) Hummelgård, M.; Zhang, R.; Nilsson, H.-E.; Olin, H. Electrical Sintering of Silver Nanoparticle Ink Studied by in-situ TEM Probing. *PLoS ONE* **2011**, *6*, e17209.

(34) Iijima, S.; Ajayan, P. M. Substrate and Size Effects on the Coalescence of Small Particles. *J. Appl. Phys.* **1991**, *70*, 5138-5140.

(35) Redinger, D.; Molesa, S.; Yin, S.; Farschi, R.; Subramanian, V. An Ink-Jet-Deposited Passive Component Process for RFID. *IEEE Trans. Electron Devices*, **2004**, *51*,1978-1983.

(36) Menicanin, A. B.; Zivanov, L. D.; Damnjanovic, M. S.; Maric, A. M. Low-Cost CPW Meander Inductors Utilizing Ink-Jet Printing on Flexible Substrate for High-Frequency Applications. *IEEE Trans. Electron Devices*, **2013**, *60*, 827-832.

(37) McKerricher, G.; Perez, J. G.; Shamim, A. Fully Inkjet Printed RF Inductors and Capacitors Using Polymer Dielectric and Silver Conductive Ink With Through Vias. *IEEE Trans. Electron Devices*, **2015**, *62*, 1002-1009.

(38) Cook, B. S.; Mariotti, C.; Cooper, J. R.; Revier, D.; Tehrani, B. K.; Aluigi, L.; Roselli, L.; Tantzeris, M. M. Inkjet-printed, Vertically-integrated, High-performance Inductors and Transformers on Flexible LCP Substrate, *International Microwave Symposium (IMS) IEEE International* **2014**, 1-4

(39) Jan, C.-H.; Agostinelli, M.; Buehler, M.; Chen, Z.-P.; Choi, S.-J.; Curello, G.; Deshpande, H.; Gannavaram, S.; Hafez, W.; Jalan, U.; Kang, M.; Kolar, P.; Komeyli, K.; Landau, B.; Lake, A.; Lazo, N.; Lee, S.-H.; Leo, T.; Lin, J.; Lindert, N.; Ma, S.; McGill, L.; Meining, C.; Paliwal, A.; Park, J.; Phoa, K.; Post, I.; Pradhan, N.; Prince, M.; Rahman, A.; Rizk, J.; Rockford, L.; Sacks, G.; Schmitz, A.; Tashiro, H.; Tsai, C.; Vandervoorn, P.; Xu, J.; Yang, L.; Yeh, J.-Y.; Yip, J.; Zhang, K.; Zhang, Y.; Bai, P. A 32nm SoC Platform Technology with 2nd Generation High-k/Metal Gate Transistors Optimized for Ultra Low Power, High Performance, and High Density Product Applications, *Electron Devices Meeting (IEDM), IEEE International* **2009**, 1-4.

(40) High Q-multilayer Chip Inductor for High Frequency Applications," Taiyo Yuden Corp., Product Data Sheet, Oct. **2011**.

(41) Frickey, D. A. Conversions Between S, Z, Y, H, ABCD, and T Parameters which are Valid for Complex Source and Load Impedances. *IEEE Trans. Microwave Theory Technology* **1994**, *42*, 205-211.

## Table of Contents (TOC) Image